Liquid Structure and Preferential Solvation of Metal Ions in Solvent Mixtures of *N*,*N*-Dimethylformamide and *N*-Methylformamide

Kenta Fujii,[†] Takashi Kumai,[‡] Toshiyuki Takamuku,[‡] Yasuhiro Umebayashi,[†] and Shin-ichi Ishiguro*[,†]

Department of Chemistry, Faculty of Science, Kyushu University, Hakozaki, Higashi-ku, Fukuoka 812-8581, Japan, and Department of Chemistry and Applied Chemistry, Faculty of Science and Engineering, Saga University, Honjo-machi, Saga 840-8502, Japan

Received: September 2, 2005; In Final Form: November 7, 2005

Raman spectra of aprotic *N*,*N*-dimethylformamide (DMF) and protic *N*-methylformamide (NMF) mixtures containing manganese(II), nickel(II), and zinc(II) perchlorate were obtained, and the individual solvation numbers around the metal ions were determined over the whole range of solvent compositions. Variation profiles of the individual solvation numbers with solvent composition showed no significant difference among the metal systems examined. In all of these metal systems, no preferential solvation occurs in mixtures with DMF mole fraction of $x_{DMF} < 0.5$, whereas DMF preferentially solvates the metal ions at $x_{DMF} > 0.5$. The liquid structure of the mixtures was also studied by means of small-angle neutron scattering (SANS) and low-frequency Raman spectroscopy. SANS experiments demonstrate that DMF molecules do not appreciably self-aggregate in the mixtures over the whole range of solvent composition. Low-frequency Raman spectroscopy suggests that DMF molecules are extensively hydrogen-bonded with NMF in NMF-rich mixtures, whereas NMF molecules extensively self-aggregate in DMF-rich mixtures, although the liquid structure in neat NMF is partly ruptured. The bulk solvent structure in the mixtures thus varies with solvent composition, which plays a decisive role in developing the varying profiles of the individual solvation numbers of metal ions in the solvent mixtures.

Introduction

Liquid structures of amides and their solvation structures around metal ion have so far been extensively studied in view of the electron-pair-donating and hydrogen-bonding abilities of the solvents. The structuredness of an amide in the liquid state changes depending on its hydrogen-bonding ability, i.e., it is strong for protic amides but weak for aprotic ones. *N*,*N*-Dimethylformamide (DMF), a typical aprotic amide without the −NH proton, is thus less-structured with only weak dipole−dipole interactions in the bulk.[1−7] *N*-Methylformamide (NMF), a typical protic amide with the −NH proton, is highly structured to form chainlike and/or ring structures through intermolecular −NH···O═C− hydrogen bonds.[8−21] Studies on the liquid structure are still ongoing, and a report of neutron scattering experiments using fully deuterated liquid NMF was recently published.[22] Theoretical studies of the liquid structure of amides[23−26] and their solvation with metal ions[27,28] have also been carried out by means of molecular dynamics simulations.

Metal-ion solvation is weaker in protic solvents than in aprotic solvents, as hydrogen bonds among protic solvent molecules are ruptured upon ion solvation. Indeed, the enthalpies of transfer, $\Delta_t H°$, of alkali and divalent transition metal ions from DMF to NMF are positive, indicating that the solvation of these ions in protic NMF is weaker than that in aprotic DMF.[29,30] On the other hand, metal(II)−halogeno complexation is significantly enhanced in DMF over NMF,[31−34] which is ascribed to positive and larger formation entropies in DMF than NMF. This cannot be explained simply in terms of ion−solvent interactions, i.e., the electron-pair-donating abilities of these solvents are almost the same, and the electron-pair-accepting ability of NMF is higher than that of DMF.[35,36] The entropy difference in the metal-ion complexation can be explained as follows: The freedom of motion of solvent molecules, both DMF and NMF, bound to a metal ion is strongly restricted, i.e., the entropy is low. On the other hand, the freedom of motion of solvent molecules in the bulk depends on the extent of solvent−solvent interaction, i.e., it is high in less-structured DMF but low in structured NMF. Upon complexation between metal and ligand ions, solvent molecules desolvate ions and are then accommodated in the bulk solvent structure. The change in freedom of motion of solvent molecules is thus large, or the entropy increase is large, in less-structured DMF, whereas it is small, or the entropy increase is moderate, in structured NMF.

Protic−aprotic solvent mixtures such as DMF−NMF mixtures can thus be particularly interesting in view of solvent structure, as DMF terminates and thus ruptures the chainlike structure of NMF. According to ^{1}H NMR spectroscopy,[37] DMF−NMF mixtures can be regarded as almost ideal mixtures over the whole range of solvent compositions. However, little is known about the liquid structure and ion solvation in DMF−NMF mixtures. Although the liquid structure of binary or ternary solvent mixtures involving DMF or NMF has been studied by means of molecular dynamics simulations,[38−40] the mixed-solvent systems always involved water as a component. According to our recent study,[41] the formation of $CoCl^+$ in DMF−NMF mixtures is significantly enhanced with increasing DMF content. This is ascribed to the increasing formation entropy,

* To whom correspondence should be addressed. E-mail: analsscc@mbox.nc.kyushu-u.ac.jp.
[†] Kyushu University.
[‡] Saga University.

10.1021/jp054972a CCC: $33.50
Published on Web 01/05/2006

implying that the liquid structure weakens with increasing DMF content. In DMF−NMF mixtures, because the two components have almost the same electron-pair-donating ability, both solvents might simultaneously solvate the metal ion. Here, note that not only ion−solvent interactions but also solvent−solvent interactions in the coordination sphere of the metal ion and in the bulk can play a role in determining the individual solvation number, or the number of molecules of each solvent component bound to the metal ion. However, such established techniques for determining the total solvation number as large-angle X-ray scattering and extended X-ray absorption fine structure (EXAFS) spectroscopy cannot be applied for the individual solvation numbers in mixtures if the two solvents involve the same or similar atoms coordinating to the metal ion. Therefore, we developed a Raman spectroscopic technique to distinguish two solvent components. This procedure has been successful in elucidating the individual solvation number of a series of first transition metal ions in DMF−*N*,*N*-dimethylacetamide mixtures.[42,43] However, individual solvation number in DMF−NMF mixture have not yet been investigated.

Here, the individual solvation numbers of manganese(II), nickel(II), and zinc(II) ions in DMF−NMF mixtures are discussed particularly in view of the liquid structure of the mixture.

Experimental Section

Reagents. DMF and NMF solvates of manganese(II), nickel(II), and zinc(II) perchlorates were prepared by dissolving their hydrates in these solvents and purified by repeated recrystallization. The DMF and NMF solvate crystals thus obtained were dried in a vacuum oven at 327 K and kept in a desiccator over P_2O_5. The number of DMF or NMF molecules per metal ion was found to be 6.0 in all of the solvate crystals by EDTA titration. NMF was dried over 3-Å molecular sieves for several weeks and further dried with barium oxide for 24 h before distillation. The NMF thus obtained was distilled at 328 K under reduced pressure (3 mmHg) and stored in a dark bottle with a P_2O_5 drying tube. DMF was dried over 4-Å molecular sieves for several weeks and distilled at 303 K under reduced pressure. The water content was verified to be negligible by Karl-Fisher titration. All materials and solutions were treated in a glovebox under an atmosphere of argon.

Raman Spectroscopy. Raman spectra were measured over the range 550−1000 cm^{-1} using a dispersion Raman spectrometer (JASCO NR-1100) with an argon ion laser (Coherent Inova 70) operating at 514.5 nm. The optical resolution was either 2.5 or 5.0 cm^{-1}. As no significant difference was found in the evaluation of the solvation number, data obtained with the optical resolution of 5.0 cm^{-1} were used for the analyses. A solvent mixture containing 0.6−0.7 mol kg^{-1} metal(II) perchlorate was titrated with a mixture of the same solvent composition without electrolyte using an autoburet (KEK APB-410), and spectral data were recorded on a personal computer at each titration point. The Raman spectra were deconvoluted into single bands. A single Raman band is assumed to be represented as a pseudo-Voigt function, $f_V(\nu) = \gamma f_L(\nu) + (1 - \gamma) f_G(\nu)$, where $f_L(\nu)$ and $f_G(\nu)$ represent Lorentzian and Gaussian components, respectively, and the parameter γ ($0 < \gamma < 1$) is the fraction of the Lorentzian component. A nonlinear least-squares curve-fitting procedure was employed for the analyses. The intensity I of a single Raman band is evaluated according to the expression $I = \gamma I_L + (1 - \gamma) I_G$, where I_L and I_G denote the integrated intensities of the Lorentzian and Gaussian components, respectively.

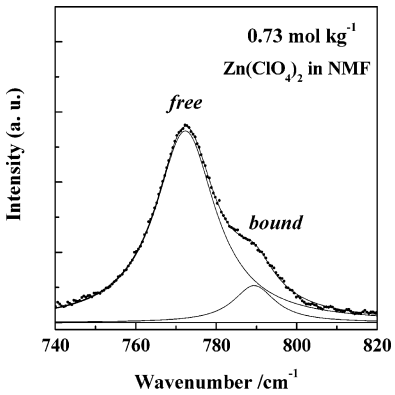

Figure 1. Typical result of deconvolution of the δ(O═C−N) vibration of NMF in the zinc(II) system.

Raman spectra in the low-frequency region of 10−400 cm^{-1} were obtained with an optical resolution of 2.0 cm^{-1} and a laser power of 500 mW. Neat DMF (or NMF) in a vessel was mixed with neat NMF (or DMF) using an autoburet (KEK APB-410), and spectral data were recorded on a personal computer at each titration point. $R(\nu)$ spectra were obtained from measured $I(\nu)$-spectra according to the equation

$$R(\nu) \propto I(\nu)(\nu_0 - \nu)^{-4}\nu[1 - \exp(-hc\nu/kT)] \qquad (1)$$

where ν_0 and ν (cm^{-1}) represent frequencies of the irradiated laser light and Raman shift, respectively, and the other parameters are physical constants or quantities of usual meanings. The $R(\nu)$ spectra were then deconvoluted into single components of a pseudo-Voigt function.

Small-Angle Neutron Scattering Measurements. Sample solutions were prepared by mixing deuterated DMF-d_7 with undeuterated NMF to obtain a high contrast of scattering for DMF. Small-angle neutron scattering (SANS) measurements for mixtures with DMF mole fractions of $x_{DMF} = 0.1-0.9$ were carried out using a SANS−U spectrometer installed on a JRR-3M reactor (JAERI, Tokai, Japan). The covered range of momentum transfer Q [$= 4\pi\lambda^{-1} \sin\theta$, where λ and 2θ denote the wavelength (7 Å) of neutron beams and the scattering angle, respectively] with the camera length of 2 m was 0.02−0.15 Å. Transmission was measured with a ^{3}He detector located at a beam stopper position. Measurements were carried out at 298.2 ± 0.1 K, and the obtained SANS intensities were corrected for the background of an empty cell and normalized with respect to the scattering of lupolen.[44] The normalized intensities were further corrected by subtraction of the incoherent scattering.

Result and Discussion

Solvation Number in Neat NMF. Figure 1 shows a typical Raman spectrum for the in-plane bending δ(O═C−N) vibration of NMF observed in a solution containing 0.73 mol kg^{-1} zinc(II) perchlorate. The δ(O═C−N) vibration at 770 cm^{-1} in the bulk (free NMF) shifts to a higher frequency upon binding to the metal ion. The sideband is thus ascribed to the solvent bound to the metal ion (bound NMF). The observed spectrum was deconvoluted into two bands, and the frequency shift, $\Delta\nu = \nu_{bound} - \nu_{free}$, was evaluated. As seen in Table 1, the magnitude of shift increases in the order Mn < Zn < Ni, the order of decreasing ionic radius of the metal ion.

Typical Raman spectra of NMF containing zinc(II) perchlorate at varying molalities are shown in Figure 2 in the ranges of 740−820 and 890−1000 cm^{-1}. With increasing salt molality, the intensity of the 770 cm^{-1} band decreases without an

TABLE 1: Coordination Number, n; Raman Scattering Coefficients of the Bulk, J_f, and Bound, J_b, Solvents; and Band Shift, $\Delta\nu$ ($\nu_{bound} - \nu_{free}$), for Manganese(II), Nickel(II), and Zinc(II) Ions[a]

solvent	x_{DMF}	n	J_f	J_b	$\Delta\nu$
		Mn(II)			
NMF	0	5.9 (0.6)	0.03	0.01	13.4
DMF	0.25	1.6 (0.1)	0.16	0.11	19.6
DMF	0.5	3.2 (0.1)	0.17	0.15	22.0
DMF	0.75	5.6 (0.1)	0.17	0.13	24.5
DMF	1[b]	6.1 (0.3)	0.16	0.15	26.2
		Ni(II)			
NMF	0	5.8 (0.3)	0.02	0.01	23.6
DMF	0.25	1.3 (0.1)	0.18	0.12	31.5
DMF	0.5	3.3 (0.1)	0.18	0.13	32.4
DMF	0.75	5.3 (0.1)	0.17	0.10	34.8
DMF	1[c]	5.8 (0.2)	0.17	0.13	36.7
		Zn(II)			
NMF	0	5.7 (0.4)	0.02	0.01	17.8
DMF	0.25	1.2 (0.1)	0.16	0.06	24.2
DMF	0.4	2.3 (0.1)	0.17	0.07	26.9
DMF	0.5	3.5 (0.1)	0.17	0.05	27.7
DMF	0.65	4.6 (0.3)	0.18	0.09	28.9
DMF	0.75	5.5 (0.1)	0.17	0.09	30.0
DMF	1[b]	5.8 (0.3)	0.17	0.12	32.7

[a] Values in parentheses are standard deviations. [b] Reference 42. [c] Reference 43.

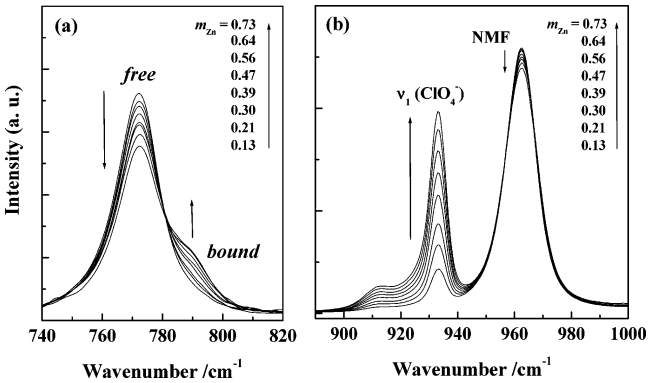

Figure 2. Raman spectra in the ranges (a) 740−820 and (b) 890−1000 cm^{-1} obtained for zinc(II) perchlorate NMF solutions with varying salt molality.

appreciable change in the peak frequency or half-width at half-maximum (HWHM). The intensity was normalized using the 933 cm^{-1} (ν_1) band of the perchlorate ion as an internal standard. The spectrum in Figure 2b also includes bands at 963 and 915 cm^{-1} originating from NMF [stretching ν(N−CH_3) and ν(CO−NH) vibrations][45] and the perchlorate ion (overtone of ν_2 at 455 cm^{-1}), respectively. The band shape of ν_1 of the perchlorate ion in NMF is rather asymmetric with a weak shoulder at the lower-frequency side. The same is also observed in water, but not in DMF, *N*,*N*-dimethylacetamide, or *N*,*N*-dimethylpropionamide.[47] Ion-pair formation of the perchlorate ion is hardly expected, because this generally shifts the band toward a higher-frequency side.[46] Although the reason the ν_1 vibration splits into two bands in protic NMF is not clear at present, the observed spectrum over the range 890−1000 cm^{-1} was deconvoluted, and the total intensity of the 933 cm^{-1} (main and shoulder) band was used for normalization of the measured Raman bands. On the basis of the normalized intensity of free NMF, the solvation number n of the metal ion in neat NMF was evaluated.

The integrated intensity of the free band is represented as $I_f = J_f m_f$, where J_f and m_f represent the Raman scattering coefficient and molality, respectively, of free NMF in the bulk.

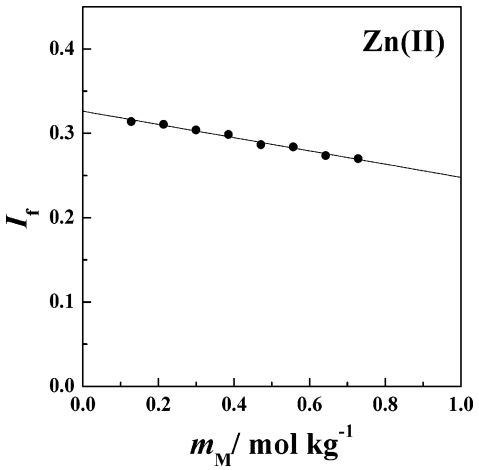

Figure 3. Typical I_f vs m_M plots for the δ(O═C−N) vibration of NMF in the zinc(II) system.

As $m_f = m_T - nm_M$, where m_T and m_M denote the total molalities of the solvent and the metal ion, respectively, in solution, we obtain the equation

$$I_f = -nJ_f m_M + J_f m_T \quad (2)$$

Because m_T is known, plots of I_f against m_M give a straight line with the intercept $\alpha = J_f m_T$ and the slope $\beta = -nJ_f$. The J_f value and the solvation number n are thus obtained as $J_f = \alpha/m_T$ and $n = -\beta/J_f$. The detailed procedure of the analyses is described elsewhere.[42,43] A typical I_f vs m_M plot for the zinc(II) system in NMF is depicted in Figure 3. The Raman scattering coefficient J_b for a bound solvent band is obtained according to $J_b = \eta/n$ using the η value given as the slope of I_b vs m_M plots ($I_b = nJ_b m_M$). The solvation numbers of the metal ions in NMF thus obtained are listed in Table 1, together with the J_f and J_b values. As seen, the solvation numbers are essentially 6 for all of the metal systems examined in NMF, as well as DMF. This is expected because NMF has an electron-pair-donating ability and a molecular structure around the coordinating carbonyl oxygen atom similar to those of DMF.

Individual Solvation Numbers in DMF−NMF Mixtures. Raman spectra of manganese(II), nickel(II), and zinc(II) perchlorate solutions in DMF have been reported previously.[42,43] The band at 660 cm^{-1} of the in-plane bending δ(O═C−N) vibration of DMF in the bulk shifts to a higher frequency upon binding of DMF to the metal ions in the order Mn < Zn < Ni, the order of decreasing ionic radius of the metal ions. The solvation numbers were obtained according to the analysis procedure described in the previous section. It has been established that the solvation number in DMF is 6 for these metal ions, the same value as obtained by means of EXAFS spectroscopy.[48]

Raman spectra for the δ(O═C−N) vibration of DMF and NMF in DMF−NMF mixtures ($x_{DMF} = 0.5$) containing metal(II) perchlorates at varying molalities are shown in Figure 4. For all of the metal systems examined, the intensity of the free solvent band decreases, and that of the bound solvent band increases without any appreciable change in the peak frequency or HWHM. The peak frequency of the bound band, on the other hand, depends strongly on the solvent composition, as shown in Table 1. The $\Delta\nu_{DMF}$ value decreases, or the metal−O(DMF) bond weakens, with decreasing x_{DMF} for all the metal system examined, whereas the $\Delta\nu_{NMF}$ value remains constant. This could be expected, because the electron-pair-donating ability of NMF is slightly larger than that of DMF.

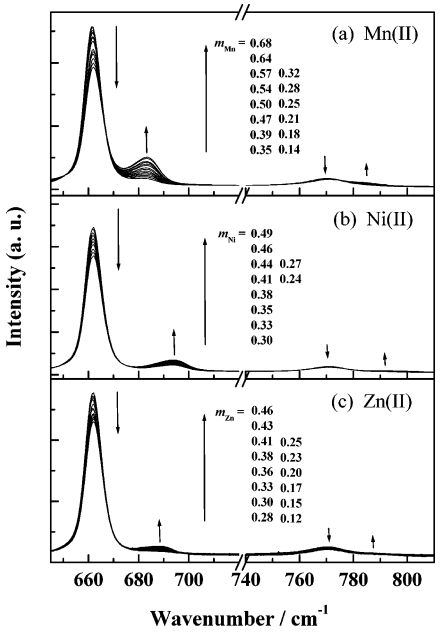

Figure 4. δ(O═C−N) vibration of DMF and NMF in a DMF−NMF mixture ($x_{DMF} = 0.5$) containing (a) $Mn(ClO_4)_2$, (b) $Ni(ClO_4)_2$, and (c) $Zn(ClO_4)_2$ at varying molalities.

The 660 cm^{-1} band of free DMF was used to determine the DMF solvation numbers in DMF−NMF mixtures. The intensity of the band was normalized using the asymmetric ν_1 band of the perchlorate ion, as in neat NMF. As seen in Table 1, the Raman scattering coefficient J_f for the 660 cm^{-1} band of free DMF thus evaluated from the asymmetric ν_1 band in the mixtures is practically the same as that evaluated from the symmetric ν_1 band in neat DMF. For all of the metal(II) systems examined, I_f vs m_M plots of the 660 cm^{-1} band of DMF in a given solvent mixture fell on a straight line, and the individual solvation numbers of DMF, n_{DMF}, were determined. (The I_f vs m_M plots are available as Supporting Information.) The values thus obtained are listed in Table 1, together with J_f and J_b values. On the other hand, as seen in Figure 4, the δ(O═C−N) vibration of NMF is too weak to evaluate the NMF solvation number in mixtures with accuracy.

The J_f values in the mixture are practically the same as that in neat DMF over the whole range of solvent compositions, suggesting that the polarity of DMF is not appreciably changed, even though DMF is strongly hydrogen-bonded with NMF in the mixture. As the solvation number of the metal ion is 6 for all of the metal systems examined in both DMF and NMF, we assumed that the total solvation number also remains 6 in the mixtures, and we calculated the mole fraction of DMF in the coordination sphere of the metal ion from $x_{DMF}^{bound} = n_{DMF}/6$. The value of x_{DMF}^{bound} in the coordination sphere is plotted against x_{DMF} in the bulk in Figure 5. As seen, no appreciable difference in the $x_{DMF}^{bound}-x_{DMF}$ plot is observed among the metal ions, implying that no specific metal−solvent or solvent−solvent (steric) interactions are involved in the coordination sphere of the metal ion. However, note that $x_{DMF}^{bound} = x_{DMF}$ holds in NMF-rich mixtures with $x_{DMF} < 0.5$, whereas $x_{DMF}^{bound} > x_{DMF}$ in DMF-rich mixtures with $x_{DMF} > 0.5$. This cannot be explained simply in terms of the electron-pair-donating ability of solvent, i.e., the ability is even slightly larger for NMF. The liquid structure of solvent, or the solvent−solvent interactions in the bulk, seems to play an essential role in the preferential solvation in DMF-rich mixtures.

Liquid Structure of DMF−NMF Mixtures. The SANS intensity, $I_{corr}(Q)$, provides information about the distribution

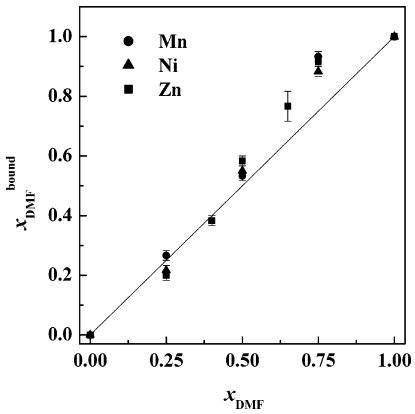

Figure 5. x_{DMF}^{bound} vs x_{DMF} plots for manganese(II), nickel(II), and zinc(II) ions.

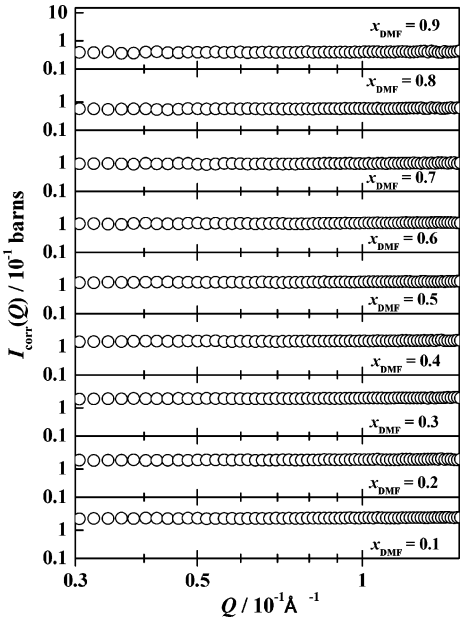

Figure 6. SANS intensities $I_{corr}(Q)$ obtained in DMF-d_7−NMF mixtures.

of molecules, homo- or heterogeneous, in solvent mixtures at the mesoscopic level. SANS techniques have been applied to some organic solvent−D_2O mixtures.[49−52] $I_{corr}(Q)$ is represented as $I_{corr}(Q) = I_0[1-(L_D^2/6)Q^2]$ in a small-Q range, where I_0 is the scattering intensity at $Q = 0$ Å^{-1} and L_D the Debye correlation length,[53] which reflects an average size of aggregates. Observed values of $I_{corr}(Q)$ in DMF-d_7−NMF mixtures are shown in Figure 6. As seen, $I_{corr}(Q)$ is practically constant, i.e., $L_D \approx 0$ Å, in the mixture over the range entire examined, $0.1 \leq x_{DMF} \leq 0.9$. This indicates that DMF does not appreciably self-aggregate, i.e., solvent molecules are homogeneously mixed in the DMF−NMF mixture at any solvent composition. This conclusion is consistent with that obtained by ^{1}H NMR spectroscopy.[39]

Low-frequency Raman spectra in the range 10−200 cm^{-1} provide information on restricted motion (translation or libration) of a molecule under the influence of intermolecular interactions of various types.[6,9,54−57] Low-frequency Raman spectra have extensively been studied for water and water−organic solvent mixtures. Liquid water shows two broad bands at 190 and 60 cm^{-1}, which are ascribed to a restricted translation of hydrogen-bonded water molecules and a frustrated translation of a water molecule accommodated in a so-called cage formed by its neighbors, respectively.[58−60] $R(\nu)$ spectra obtained for DMF−

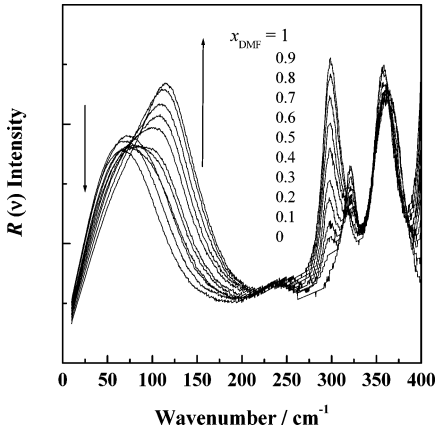

Figure 7. Reduced Raman spectra $R(\nu)$ obtained in DMF−NMF mixtures.

NMF mixtures are shown in Figure 7. The $R(\nu)$ spectrum for neat NMF exhibits two broad peaks at around 50 and 117 cm^{-1}, similarly to water. These bands are assigned to intermolecular librations.[19,25] On the other hand, the $R(\nu)$ spectrum for neat DMF shows a single band at 66 cm^{-1}. It is thus proposed that the higher-frequency band corresponds to the libration of hydrogen-bonded solvent molecules and the lower-frequency band corresponds to the libration of solvent molecules accommodated in a cage formed by neighbors. According to our recent study, two Raman bands for NMF, as well as water, and a single band for DMF in the range <200 cm^{-1} have indeed been reproduced by means of molecular dynamics simulations using 256 solvent molecules.

$R(\nu)$ spectra in Figure 7 obtained at varying solvent compositions of the DMF−NMF mixture show isosbestic points for intramolecular vibrational bands observed in the range >200 cm^{-1}. This does not apply for bands in the range <200 cm^{-1}. The 117 cm^{-1} band (higher-frequency band) in neat NMF shifts slightly and gradually with increasing x_{DMF}, implying that NMF is hydrogen-bonded to DMF to give a shifted band. A similar behavior is also seen for the 50 cm^{-1} band (lower-frequency band) in neat NMF, which gradually shifts with increasing x_{DMF}, implying that NMF is accommodated in a newly developed cage involving DMF molecules to give a shifted band. The shifted band might thus reflect formation of a new type of liquid structure or intermolecular interaction in the DMF−NMF mixture. Indeed, it is difficult to simultaneously reproduce all $R(\nu)$ spectra of the mixtures with a limited number of intrinsic bands. Thus, the $R(\nu)$ spectrum for a given mixture was deconvoluted into two bands, and the peak frequency ν, HWHM ω, and intensity I of each band were obtained. A typical $R(\nu)$ spectrum for a 1:1 mixture and its deconvoluted bands are shown in Figure 8, together with those for neat DMF and NMF.

The variation profiles of ν, ω, and I in Figure 9 show a characteristic feature, i.e., each parameter value varies linearly with x_{DMF}, and the slope in the NMF-rich mixtures is appreciably different from that in the DMF-rich mixtures. Considering the higher-frequency band, the ν value shifts monotonically to a lower frequency with increasing x_{DMF} in the NMF-rich mixtures, but remains ca. 110 cm^{-1} in the DMF-rich mixtures. As discussed above, the higher-frequency band originates from the libration of hydrogen-bonded NMF; the ν shift in the NMF-rich mixture can be explained in terms of rupture of the chainlike structure of self-aggregated NMF and formation of NMF hydrogen-bonded to DMF. Furthermore, the ν value, which remains constant in the DMF-rich mixtures, implies that the formation of self-aggregated NMF is strongly suppressed but

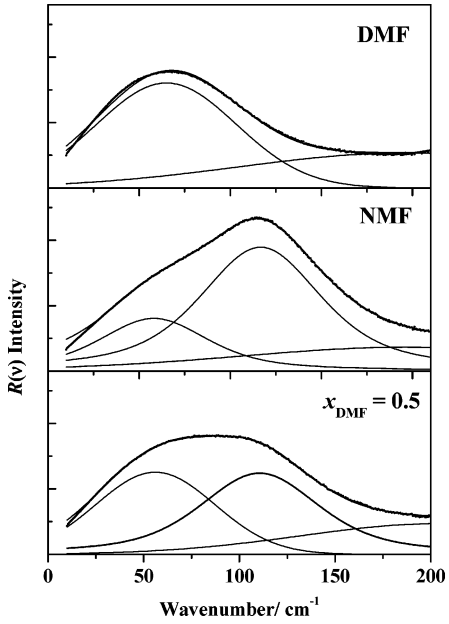

Figure 8. Typical results of deconvolution of $R(\nu)$ spectra obtained in neat DMF, neat NMF, and a 1:1mixture.

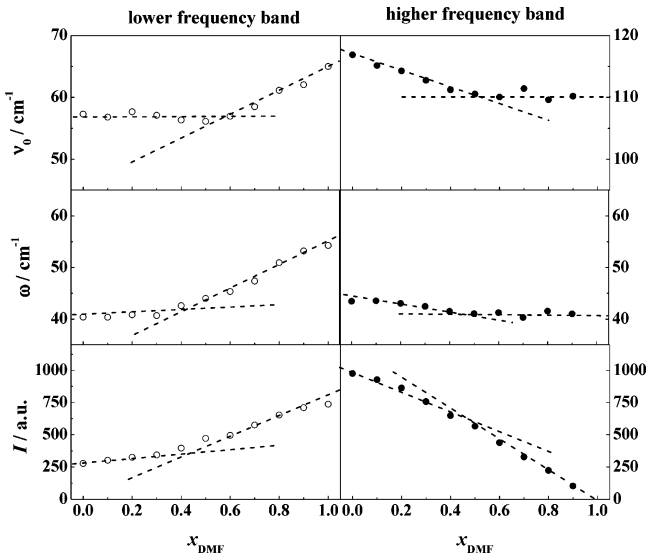

Figure 9. Variation of peak frequency ν_0, half-width at half-maximum ω, and intensity I of bands appearing at higher and lower frequencies in the range <200 cm^{-1} with the DMF content x_{DMF} in DMF−NMF mixtures.

NMF is extensively hydrogen-bonded with DMF in mixtures with $x_{DMF} > 0.5$. It is thus proposed that the 110 cm^{-1} band be ascribed to NMF hydrogen-bonded to DMF. The intensity decreases monotonically with x_{DMF} to approach zero at $x_{DMF} = 1$. This can also be explained in terms of the rupture of the chainlike structure of self-aggregated NMF and the formation of hydrogen bonds between NMF and DMF. The intensity decrease is even enhanced with increasing x_{DMF}, implying that the Raman scattering coefficient for self-aggregated NMF is smaller than that for NMF hydrogen-bonded to DMF.

The strong tendency of DMF to rupture the chainlike structure of self-aggregated NMF is also evidenced by the lower-frequency band, which provides information on frustrated libration of either DMF or NMF molecules accommodated in a cage formed by its neighbors. The 55 cm^{-1} band does not shft appreciably, and its HWHM, ω, in neat NMF remains almost unchanged in NMF-rich mixtures. The corresponding band for

DMF−DMF interactions in neat DMF appears at 66 cm^{-1}. This implies that no DMF−DMF interactions are involved, or that DMF is homogeneously dispersed, in NMF-rich mixtures.

Individual Solvation Number and Solvent Structure. The work reported herein revealed that the manganese(II), nickel(II), and zinc(II) ions are six-coordinate in neat NMF, as well as in neat DMF. This might apply as well in DMF−NMF mixtures. As described in the previous section, if only the metal−solvent interaction is taken into account, no preferential solvation of the metal(II) ion is expected in the mixtures. Indeed, the metal ion is not preferentially solvated in mixtures with $x_{DMF} < 0.5$. However, the metal ions evidently prefer DMF to NMF in DMF-rich mixtures. This cannot be explained without taking into account the liquid structure in DMF−NMF mixtures.

Let us consider the process of solvation of a metal ion in the gas phase into a DMF−NMF mixture. In an NMF-rich mixture, DMF molecules are hydrogen-bonded with NMF, and excess NMF molecules extensively self-aggregate to form a chainlike structure. When the metal ion is introduced into the mixture, solvent−solvent bonds, either DMF−NMF or NMF−NMF, are ruptured, and the liberated molecules then solvate the metal ion. Here, note that, because DMF and NMF have similar electron-pair-donating abilities, the energies required to rupture NMF−DMF and NMF−NMF hydrogen bonds are not significantly different. This might be the reason preferential solvation of the metal ion does not occur in NMF-rich mixtures with $x_{DMF} < 0.5$. On the other hand, in DMF-rich mixtures with $x_{DMF} > 0.5$, NMF molecules are extensively hydrogen-bonded with DMF, whereas excess DMF molecules are free from hydrogen bonding. When the metal ion is introduced into such a mixture, the hydrogen-bonded NMF needs to rupture strong intermolecular bonds, unlike the non-hydrogen-bonded DMF. This might lead to preferential solvation of the metal ion with DMF in DMF-rich mixtures.

Consequently, we propose that the liquid structure of the solvent is responsible for preferential solvation in DMF−NMF mixtures and that no specific metal−solvent interactions are involved in the metal−solvent systems examined. This might lead to $x_{DMF}^{bound}-x_{DMF}$ plots that are independent of the metal ion, as is, in fact, seen for the metal ions examined here.

Conclusion

Manganese(II), nickel(II), and zinc(II) ions are all six-coordinate in neat NMF and DMF. The same total solvation number is proposed also in DMF−NMF mixtures. The individual DMF solvation numbers of these metal ions in the mixtures were obtained by Raman spectroscopy. The results revealed that no preferential solvation of these metal(II) ions occurs in NMF-rich mixtures, whereas DMF is preferred in DMF-rich mixtures. Also, no appreciable difference among metal ions is found in the $x_{DMF}^{bound}-x_{DMF}$ plots. The liquid structure of the DMF−NMF mixture was investigated by means of SANS measurements and low-frequency Raman spectroscopy. These studies revealed that solvent molecules are homogeneously mixed in the mixtures over the whole range of solvent compositions. In NMF-rich mixtures, DMF is extensively hydrogen-bonded with NMF, and excess NMF molecules self-aggregate to form a chainlike structure. In DMF-rich mixtures, NMF is extensively hydrogen-bonded with DMF, and excess DMF molecules are free from hydrogen bonding. In DMF-rich mixtures, the metal ion prefers the non-hydrogen-bonded DMF to the hydrogen-bonded NMF, leading to the preferential solvation of the metal ion with DMF.

Acknowledgment. This work was financially supported by Grant-in-Aids for Scientific Research 13440222 and 15750052 from the Ministry of Education, Culture, Sports, Science and Technology of Japan and also by a Grant for Basic Science Research Project from the Sumitomo Foundation.

Supporting Information Available: The individual DMF solvation numbers of the metal ions in DMF−NMF mixtures as obtained from I_f-m_M plots (Figure S-1). This material is available free of charge via the Internet at http://pubs.acs.org.

References and Notes

(1) Rabinowitz, M.; Pines, A. *J. Am. Chem. Soc.* **1969**, *91*, 1585.
(2) Ohtaki, H.; Itoh, S.; Yamaguchi, T.; Ishiguro, S.; Rode, B. M. *Bull. Chem. Soc. Jpn.* **1983**, *56*, 3406.
(3) Radnai, T.; Itoh, S.; Ohtaki, H. *Bull. Chem. Soc. Jpn.* **1988**, *61*, 3845.
(4) Konrat, R.; Sterk, H. *J. Phys. Chem.* **1990**, *94*, 1291.
(5) Puhovski, Y. P.; Rode, B. M. *Chem. Phys.* **1995**, *190*, 61.
(6) Colaianni, S. E. M.; Nielsen, O. F. *J. Mol. Struct.* **1995**, *347*, 267.
(7) Borrmann, H.; Persson, I.; Sandstrom, M.; Stalhandske, C. M. V. *J. Chem. Soc., Perkin Trans.* **2000**, *2*, 393.
(8) Ohtaki, H.; Itoh, S.; Rode, B. M. *Bull. Chem. Soc. Jpn.* **1986**, *59*, 271.
(9) Nielsen, O. F.; Christensen, D. H.; Rasmussen, O. H. *J. Mol. Struct.* **1991**, *242*, 273.
(10) Neuefeind, J.; Chieux, P.; Zeidler, M. D. *Mol. Phys.* **1992**, *76*, 143.
(11) Neuefeind, J.; Zeidler, M. D.; Poulsen, H. F. *Mol. Phys.* **1996**, *87*, 189.
(12) Hammami, F.; Bahri, M.; Nasr, S.; Jaidane, N.; Oummezzine, M.; Cortes, R. *J. Chem. Phys.* **2003**, *119*, 4419.
(13) Hammami, F.; Nasr, S.; Oummezzine, M.; Cortes, R. *Biomol. Eng.* **2002**, *19*, 201.
(14) Bour, P.; Tam, C. N.; Sopkova, J.; Trouw, F. R. *J. Chem. Phys.* **1998**, *108*, 351.
(15) Ludwig, R.; Weinhold, F.; Farrar, T. C. *J. Chem. Phys.* **1997**, *107*, 499.
(16) Torii, H.; Tatsumi, T.; Kanazawa, T.; Tasumi, M. *J. Phys. Chem. B* **1998**, *102*, 309.
(17) Torii, H.; Tasumi, M. *J. Phys. Chem. B* **1998**, *102*, 315.
(18) Torii, H.; Tasumi, M. *Int. J. Quantum Chem.* **1998**, *70*, 241.
(19) Torii, H.; Tasumi, M. *J. Phys. Chem. A* **2000**, *104*, 4174.
(20) Bushuev,Y. G.; Davletbaeva, S. V. *Russ. Chem. Bull.* **2000**, *49*, 238.
(21) Barthel, J.; Buchner, R.; Wurm, B. *J. Mol. Liq.* **2002**, *98*, 51.
(22) Hammami, F.; Nasr, S.; Brhri, M.; Bellissemt-Funel, M. C.; Oumezzine, M. *J. Phys. Chem. B* **2005**, *109*, 16169.
(23) Gao, J.; Pavalites, J. J.; Habibollazadeh, D. *J. Phys. Chem.* **1996**, *100*, 2689.
(24) Chalaris, M.; Samios, J. *J. Chem. Phys.* **2000**, *112* (19), 8581.
(25) Puhovski, Y. P.; Safonova, L. P.; Rode, B. M. *J Mol. Liq.* **2003**, *103−104*, 15.
(26) Skarmoutsos, I.; Samios, J. *Chem. Phys. Lett.* **2004**, *384*, 108.
(27) Pukhovskii, Y. P.; Sakharov, D. V.; Safonova, L. P. *J. Struct. Chem.* **2002**, *43* (2), 284.
(28) Chalaris, M.; Samios, J. *J. Mol. Liq.* **1998**, *78*, 201.
(29) Marcus, Y. *Pure Appl. Chem.* **1985**, *57*, 1103.
(30) Męcik, M.; Chudziak, A. *J. Solution Chem.* **1985**, *14*, 653.
(31) Ishiguro, S.; Jeliazkova, B. G.; Ohtaki, H. *Bull. Chem. Soc. Jpn.* **1985**, *58*, 1143.
(32) Ishiguro, S.; Ozutsumi, K.; Ohtaki, H. *Bull. Chem. Soc. Jpn.* **1987**, *60*, 531.
(33) Ishiguro, S.; Ozutsumi, K.; Ohtaki, H. *J. Chem. Soc., Faraday Trans. 1* **1988**, *84*, 2409.
(34) Fujii, K.; Umebayashi, Y.; Kanzaki, R.; Kobayashi, D.; Matsuura, R.; Ishiguro, S. *J. Solution Chem.* **2005**, *34* (7), 739.
(35) (a) Gutmann, V.; Wychera, E. *Inorg. Nucl. Chem. Lett.* **1966**, *2*, 257. (b) Gutmann, V. *Coordination Chemistry in Nonaqueous Solutions*; Springer-Verlag: New York, 1968.
(36) Mayer, U.; Gutmann, V.; Gerger, W. *Mh. Chem.* **1975**, *106*, 1235.
(37) Kinart, C. M.; Kinart, W. J.; Kolasinski, A. *Phys. Chem. Liq.* **1998**, *36*, 133.
(38) Zielkiewicz, J. *Phys. Chem. Chem. Phys.* **2000**, *2*, 2925.
(39) Chalaris, M.; Koufou, A.; Samios, J. *J. Mol. Liq.* **2002**, *101* (1−3), 69.
(40) Lei, Y.; Li, H.; Pan, H.; Han, S. *J. Phys. Chem. A* **2003**, *107*, 1574.
(41) Fujii, K.; Kobayashi, D.; Kumai, T.; Takamuku, T.; Umebayashi, Y.; Ishiguro, S. *J. Therm. Anal. Calorim.*, manuscript submitted.

(42) Umebayashi, Y.; Matsumoto, K.; Watanabe, M.; Ishiguro, S. *Phys. Chem. Chem. Phys.* **2001**, *3*, 5475.
(43) Umebayashi, Y.; Matsumoto, K.; Watanabe, M.; Katoh, K. Ishiguro, S. *Anal. Sci*. **2001**, *17*, 323.
(44) Wignall, G. D.; Bates, F. S. *J. Appl. Cryst*. **1987**, *20*, 28.
(45) Nandini, G.; Sathyanarayana, D. N. *J. Mol. Struct. (THEOCHEM)* **2002**, *579*, 1.
(46) Miller, A. G.; Macklin, J. W. *J. Phys. Chem.* **1985**, *89*, 1193.
(47) Umebayashi, Y.; Mroz, B.; Asada, M.; Fujii, K.; Matsumoto, K.; Mune, Y.; Probst, M.; Ishiguro, S. *J. Phys. Chem. A* **2005**, *109*, 4862.
(48) Ozutsumi, K.; Koide, M.; Suzuki, H.; Ishiguro, S. *J. Phys. Chem.* **1993**, *97*, 500.
(49) Takamuku, T.; Nakamizo, A.; Tabata, M.; Yoshida, K.; Yamaguchi, T.; Otomo, T. *J. Mol. Liq.* **2003**, *103*−*104*, 143.
(50) Takamuku, T.; Yamaguchi, A.; Matsuo, D.; Tabata, M.; Yamaguchi, T.; Otomo, T.; Adachi, T. *J. Phys. Chem. B* **2001**, *105*, 10101.
(51) Yoshida, K.; Yamaguchi, T.; Adachi, T.; Otomo, T.; Matsuo, D.; Takamuku, T.; Nishi, N. *J. Chem. Phys.* **2003**, *119*, 6132.
(52) Takamuku, T.; Matsuo, D.; Yamaguchi, A.; Tabata, M.; Yoshida, K.; Yamaguchi, T.; Nagao, M.; Otomo, T.; Adachi, T. *Chem. Lett.* **2000**, 878.
(53) Debye, P. *J. Chem. Phys.* **1959**, *31*, 680.
(54) Walrafen, G. E.; Hokmabadi, M. S.; Yang, W. H. *J. Chem. Phys.* **1986**, *85*, 6970.
(55) Walrafen, G. E. *J. Phys. Chem.* **1990**, *94*, 2237.
(56) Mizoguchi, K.; Hori, Y.; Tominaga, Y. *J. Phys. Chem.* **1992**, *97*, 1961.
(57) Egashira, K.; Nishi, N. *J. Phys. Chem. B* **1998**, *102*, 4054.
(58) Idrissi, A.; Sokolic, F.; Perera, A. *J. Chem. Phys.* **2000**, *112*, 9479
(59) Idrissi, A.; Longelin, S.; Sokolic, F. *J. Phys. Chem. B* **2001**, *105*, 6004.
(60) Padro, J. A.; Marti, J. *J. Chem. Phys.* **2003**, *118*, 452.